

Hydrogen Bond vs Proton Transfer in HZSM5 Zeolite. A Theoretical Study

Xavier Solans-Monfort,^{†,||} Mariona Sodupe,^{*,†} Otilia Mó,[‡] Manuel Yáñez,^{*,‡} and José Elguero[§]

Departament de Química, Universitat Autònoma de Barcelona, Bellaterra 08193, Spain, Departamento de Química, C-9, Universidad Autónoma de Madrid, Cantoblanco, 28049 Madrid, Spain, and Instituto de Química Médica, CSIC, C/Juan de la Cierva, 3, 28006 Madrid, Spain

Received: April 13, 2005; In Final Form: July 27, 2005

The interaction of a large set of bases covering a wide range of the basicity scale with HZSM5 medium-size zeolites has been investigated through the use of two model clusters, namely 5T and 7T:63T. The 5T cluster has been treated fully ab initio at the B3LYP level, whereas the 63T cluster has been treated with the ONIOM2 scheme using the B3LYP:MNDO combination for geometry optimizations and B3LYP:HF/3-21G for adsorption energies. The optimized geometries of the different hydrogen bond (HB) and ion pair (IP) complexes obtained with both models are rather similar. However, there are significant dissimilarities as far as the adsorption energies are concerned, in particular when dealing with IP clusters whose intrinsic stability is largely underestimated when the simpler 5T model is used. 5T clusters could be used to obtain reasonable estimates of adsorption energies provided these are scaled by a factor of 1.1 for HB complexes and 1.4 for IP complexes. The zeolite cavity favors the proton transfer process, similarly to that found by third polar partners in gas-phase HB trimers. The intrinsic basicity of the base and its adsorption energy within the zeolite are correlated. From this correlation, is possible to conclude that, in general, bases with proton affinities (PA) larger than 200 kcal mol⁻¹ should lead to the formation of IPs, whereas bases with PA smaller than this value should form HB complexes.

I. Introduction

A hydrogen bond (HB) can be regarded as the incipient state of a proton transfer (PT) process from the proton donor toward the proton acceptor.^{1–3} Depending on the strength of the HB, this process follows some kind of gradation. In one of the limits, when we have an archetypal HB, as for example in FH...FH or FH...NH₃ dimers, both the HB donor and the HB acceptor retain most of their characteristics as isolated systems, and appear only slightly distorted within the dimer. When the strength of the HB increases, as is the case, for example, in ClH...NH₃ hydrogen bonded complexes, the system is better described as a quasisymmetric proton-shared HB in which the proton of the HB donor is almost midway between both heteroatoms.⁴ In the other limit, as is the case in IH...NH₃ interactions, the proton transfer is complete and the system can actually be viewed as a hydrogen-bonded I⁻...NH₄⁺ ion pair.⁴

The possibility of having a spontaneous PT has intrigued scientists for several years, and many efforts have been devoted, both from the experimental and the theoretical point of view, to put in evidence the formation of these ion pairs in the gas phase.^{4–16} It is quite obvious that a necessary condition would be to bring together a strong base (HB acceptor) and a strong acid (HB donor), and this motivated a great deal of efforts to expand both the gas-phase basicity and acidity scales.^{17–19} However, the gap between the intrinsic acidity of the proton donor and the intrinsic basicity of the proton acceptor can be as large as 100 kcal mol⁻¹, as recently shown in the literature,

for a large set of complexes between HF, HCl, and HBr and a set of bases that covered a large range of the gas-phase basicity scale.³ Also interestingly, the surrounding media can have an important enhancement effect on the PT transfer process. This explains, for example, that while in the gas phase the interaction between HBr and trimethylamine leads to conventional hydrogen-bonded complexes, in N₂ matrixes they have a clear (CH₃)₃-NH⁺-Br⁻ character.⁵

Acidic zeolites may be good systems to catalyze PT because, on one hand, they are able both to bind protons and to release them,^{20–23} and at the same time they provide a crystal-surrounding cavity that favors a spontaneous proton transfer between the Brønsted acid site and the adsorbed molecule. As a matter of fact, acidic protons in zeolites are known^{24–26} to be mobile at high temperatures, and this mobility can be catalyzed by water molecules or other chemical species that bridge the proton donor and acceptor sites.²⁷ However, despite the vast knowledge of their catalytic activity^{28–30} and the efforts made to understand their acidic properties, several aspects are still controversial. One of the reasons for this uncertainty is that the zeolite acidity is determined from indirect measurements, for example, by the adsorption of different probe molecules and the subsequent analysis of the adsorbed complexes and adsorption energies. Several techniques such as IR and NMR spectroscopies and temperature-programmed desorption and microcalorimetry experiments are used for this purpose.^{31–33} In particular, the nature of the adsorbed complex: (i) hydrogen bonded (HB) or (ii) ion pair (IP) derived from the proton transfer reaction, or even the existence of both forms, has been largely discussed^{21,34,35} because this is considered one of the key points for their catalytic activity.

Computational chemistry is a very useful tool to understand and rationalize the nature of the adsorbed complexes. However, zeolites normally present large unit cells with low symmetry

* Corresponding author. E-mail: Mariona@klngon.uab.es (M.S.) and manuel.yanez@uam.es (M.Y.).

[†] Universitat Autònoma de Barcelona.

[‡] Universidad Autónoma de Madrid.

[§] Instituto de Química Médica.

^{||} Present address LSDSMS (UMR 5636 CNRS-UM2), cc14, Institut Gerhardt, Université Montpellier II.

due to the Si/Al substitution, and thus, periodic calculations are usually computationally very demanding. This fact has encouraged several researchers to look for cost-effective approaches to model zeolites. In this context, the ONIOM scheme^{36–38} is increasingly being used in material chemistry modeling^{39–49} because the properties of the Brønsted site can be treated at a high level of theory, whereas the effects of the framework are introduced at a much lower (and less expensive) level.

The aim of this paper is to perform a systematic study of the adsorption of different probe molecules, which cover a large range of the gas-phase basicity scale, in H^+ exchanged zeolites and compare the results with those obtained for gas-phase acid–base interactions.³ In particular, we will focus on what would be the required intrinsic basicity of the probe molecule to get the IP structure. MFI is the chosen zeolite framework because it presents a large variety of industrial applications and their pores (10-membered ring channels) are medium size, which avoids some specific features of small channels. Moreover, we are also interested in analyzing the limitations of small cluster models, compared to larger ones treated using the ONIOM2 scheme, to describe the adsorption of several well-known families such as H_2O , CH_3OH , and CH_3OCH_3 or NH_3 , NH_2CH_3 , and $NH(CH_3)_2$ in HZSM5. Particularly interesting is establishing whether a scale factor can be applied to correct the adsorption energy obtained with the small clusters.

II. Computational Details

Two different strategies have been considered to model the zeolite framework (see Figure 1). The first one considers a pentatetrahedral $[Al(OSiH_3)_4H]$ cluster (5T) to represent the active site of the zeolite. In the second one, a much larger cluster (63T) is considered with the hybrid two-layer ONIOM2 scheme. This cluster includes the 10-membered ring with the appropriate constraints and extends the system around the Brønsted site with a similar number of tetrahedra. The inner layer, treated at a higher level of calculation, has seven tetrahedra (7T) that include the previous 5T plus two more tetrahedra of the 10-membered ring. Previous results for the adsorption of NH_3 and H_2O in acidic Chabasite⁵⁰ have shown that, if the inner layer includes the near environment of the acid site as well as all the oxygen atoms of the channel that may be involved in the formation of hydrogen bonds, the obtained results are essentially equal to those obtained with full periodic DFT calculations. Hereafter, this cluster is referred as 7T:63T (Figure 1b), and the total energy of the system is obtained from three independent calculations:

$$E^{ONIOM2} = E_{7T}^{high} + E_{63T}^{low} - E_{7T}^{low} \quad (1)$$

This method can be viewed as an extrapolation scheme. By starting from E_{7T}^{high} , the extrapolation to the real system $E_{63T}^{low} - E_{7T}^{low}$ is assumed to give an estimation for E_{63T}^{high} . This way the larger 63T cluster only needs to be computed at the low level of theory.

5T geometry optimizations and harmonic vibrational frequencies have been computed using the nonlocal hybrid three-parameter B3LYP density functional method^{51,52} and the Pople's 6-31++G(d,p) basis set.⁵³ 7T:63T geometries are also fully optimized because the framework geometry is expected to be well represented by the 63T cluster and partial optimizations may include too-rigid constraints. The inner part (7T) has been computed at the same B3LYP/6-31++G(d,p) level of theory, whereas for the low-level part, we have used the semiempirical method MNDO.⁵⁴ The final energy, however, has been obtained

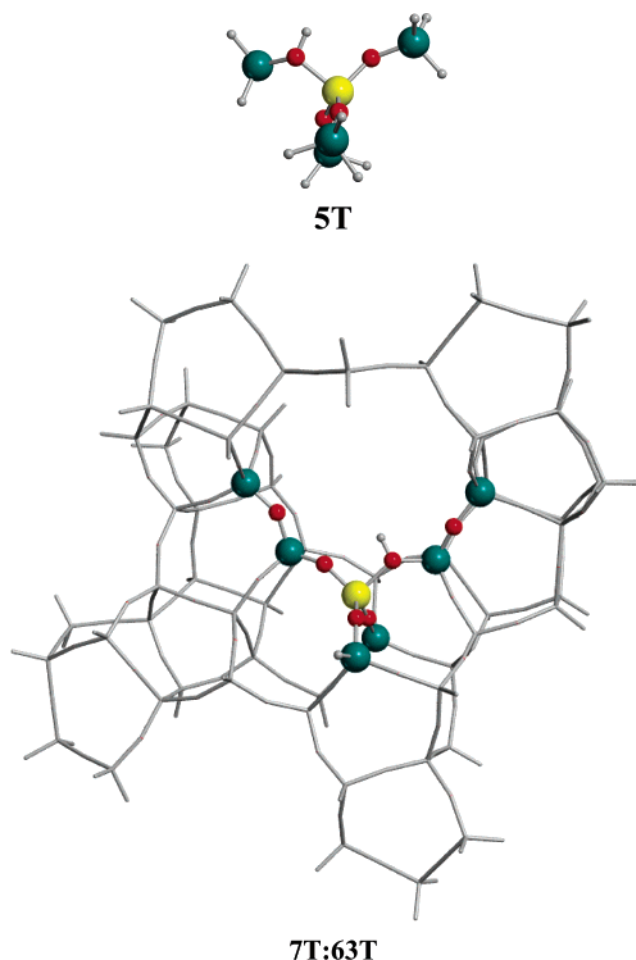


Figure 1. Cluster models (5T and 7T:63T) used to study the adsorption of probe molecules in HZSM5. Stick atoms are treated at a lower level of theory in the ONIOM2 approach.

by performing B3LYP/6-31++G(d,p):HF/3-21G single-point calculations at the optimized B3LYP/6-31++G(d,p):MNDO geometries, that is, by using HF/3-21G instead of MNDO as the low level. This methodology has been reported to describe properly the interaction energy of both hydrogen-bonded and ion pair complexes while avoiding the expensive B3LYP:HF/3-21G optimizations.⁵⁰ The good performance of this procedure has also been checked in the present study by optimizing the $NH_4^+Z^-$ (7T:63T) ion pair complex at the B3LYP/6-31++G(d,p):HF/3-21G level of theory. Results show that the B3LYP/6-31++G(d,p):HF/3-21G adsorption energies differ by less than 0.3 kcal/mol regardless of whether we use the B3LYP/6-31++G(d,p):MNDO or B3LYP/6-31++G(d,p):HF/3-21G geometries.

It should be mentioned that density functional methods do not take into account the dispersion energy. However, most of the studied probe molecules are small and interact with the acid Brønsted site of the zeolite through medium or strong hydrogen bonds, and so dispersion forces are expected to be only a minor component of the interaction. All calculations have been performed with GAUSSIAN98 package.⁵⁵

III. Results and Discussion

The adsorption energies for the 25 bases investigated obtained through the use of a 5T cluster have been summarized in Table 1. The optimized geometries of the different aggregates are given as Supporting Information. Three different subsets can be easily identified within the whole set considered: bases that only yield

TABLE 1: Proton Affinities, and Base–HZ Adsorption Energies (in kcal mol^{−1}) at the B3LYP/6-31++G(d,p) Level of Theory

species	PA	exp. PA ^a (kcal mol ^{−1})	hydrogen bond (HB)		ion pair (IP)	
			E_{ads}^b	$f^*E_{\text{ads}}^c$	E_{ads}^b	$f^*E_{\text{ads}}^c$
zeolite [−]	293.6					
NO (on O)	110.3	117.5 ^d	−1.4	−1.5		
NO (on N)	124.7	127.1	−2.3	−2.5		
CO ₂	127.0	129.2	−4.5	−5.0		
CO	140.0	142.0	−4.6	−5.1		
F ₂ CO	146.8	159.3	−5.1	−5.6		
H ₂ O	165.1	165.2	−16.3	−17.9		
CH ₃ OH	180.4	180.3	−17.0	−18.7		
CH ₃ CHO	185.2	183.7	−13.7	−15.1		
CH ₃ CN	188.1	186.2	−12.9	−14.2		
CH ₃ OCH ₃	189.1	189.3	−14.3	−15.7		
NH ₂ CHO	195.0	196.6	−21.5	−23.7		
H ₃ PO ₂	196.9	195.5 ^d	−26.7	−29.3		
CH ₃ COCHCH ₂	201.4	199.5	−14.0	−15.4		
NH ₃	204.7	204.0	−19.0	−20.9	−19.5	−27.3
CH ₂ NH	207.4	203.8	−17.2	−18.9	−15.8	−22.1
(CH ₃)CHNH	213.2	211.5	−18.4	−20.2	−19.0	−26.6
pyrazole	214.0	213.7	−24.0	−26.4	−25.2	−35.2
CH ₃ NH ₂	215.4	214.9			−24.0	−33.6
(CH ₃) ₂ NH	222.2	221.2			−26.9	−37.7
(CH ₃) ₃ N	226.3	226.8			−24.2	−33.8
(CH ₃) ₂ CNH	233.0	222.8	−24.5	−27.0	−28.4	−39.7
NH ₂ CHNH	233.6	228.5			−38.4	−53.8
ON(CH ₃) ₃	234.0	228.9 ^d			−34.5	−48.3
NH ₂ (CH ₃)CNH	241.6	232.0			−41.3	−57.8
(NH ₂) ₂ CNH	246.4	235.7			−44.5	−62.3

^a Values taken from NIST database (<http://webbook.nist.gov/chemistry/>). ^b Obtained with the 5T cluster. ^c $f = [E_{\text{ads}}(7\text{T}:63\text{T})]/E_{\text{ads}}(5\text{T})$ (see text and Table 2). ^d Values in italics were estimated from the linear correlation of Figure 3.

hydrogen-bonded complexes, bases that lead exclusively to an IP formation, and bases in which both situations are found to be local minima of the potential energy surface. It is also apparent, from the values in Table 1, that for bases which have a proton affinity (PA) more than 89 kcal mol^{−1} lower than the acidity of the zeolite, only a HB structure should be expected, while for bases with a PA which differ from the acidity of the zeolite by less than 78 kcal mol^{−1}, except (CH₃)₂CNH, only an IP is stable. For bases within these two limits, both situations appear to be rather close in energy. Nevertheless, by taking into account that the IP will be particularly favored by the interaction with the surroundings, it is mandatory to carry out a calibration of this very simple model.

Calibration of 5T Cluster. The limitations of the 5T cluster to model the adsorption of small-probe molecules in HZSM5, an example of a medium-pore-size zeolite, have been analyzed by comparing the results with those obtained with the 7T:63T cluster. We have considered 12 probe molecules out of the initial set of 25, which include different basic sites and with proton affinities ranging from 140 to 222 kcal mol^{−1}. Thus, we expect that the conclusions obtained will be general enough to be applied to any small basis adsorbed in a medium-sized zeolite.

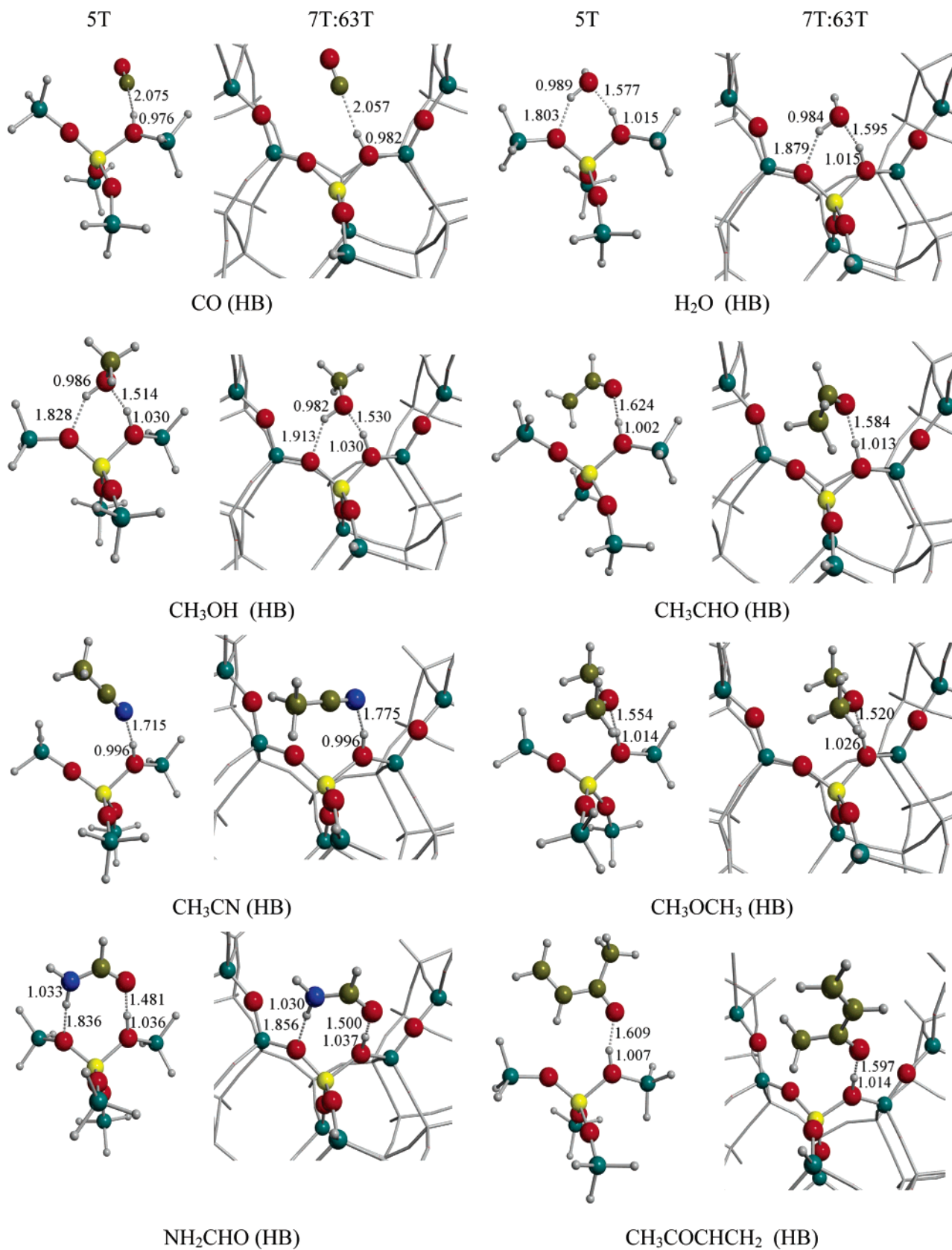
Figure 2 shows the optimized structures of the adsorbed complexes by using both the 5T and the 7T:63T clusters. The adsorption energies as well as the proton affinities of the probe molecules are given in Table 2. It can be observed that, with the two cluster models, the adsorption of molecules with proton affinities smaller than 204 kcal mol^{−1} leads to formation of a hydrogen-bonded complex, in agreement with the experimental evidence.^{21,34,35} Moreover, the optimized structures of Base–HZ obtained with HZ being 5T or 7T:63T are very similar. In

particular, it is noticeable that, in all cases, the two models provide the same kind of hydrogen bonds between the base molecule and the zeolite; that is, in all cases, the oxygen atoms of the zeolite framework involved in the HB are those directly bonded to aluminum. The largest variation of the hydrogen bond distance involving the Brønsted acid site upon enlarging the cluster model is ~ 0.06 Å. Not unexpectedly, larger variations are observed for the weaker hydrogen bonds in which the oxygen atoms of the zeolite act as proton acceptor. It should be noted that the basicity of the zeolite oxygen atoms depends on the SiOAl angle, which is much more constrained in the larger 7T:63T cluster. The main differences between the 5T and 7T:63T optimized geometries occur for acetaldehyde, acetonitrile, and butenone, which show a different orientation upon interacting with the Brønsted site. This is probably related to the fact that the 7T:63T cluster includes the 10-membered ring, which introduces larger steric repulsion between the probe molecule and the zeolite framework. However, we expect that this change in orientation will not significantly alter the adsorption energy of these systems.

As mentioned above, the adsorption of NH₃ and CH₂NH leads to both HB and IP structures when the 5T model is used, and the energy difference between the two structures is only -0.5 and 1.4 kcal/mol, respectively. However, because the zeolite framework stabilizes the IP structure more than the HB one, calculations with the larger 7T:63T cluster provide the IP structure to be the global minimum in both cases. Moreover, for NH₃, the HB structure appears not to be stable because all attempts to optimize such a structure collapsed to the IP one. For CH₂NH, the two structures are found to be stable, but in thermodynamic conditions, the population of the HB will be lower than 1%. Experimentally, it is expected that molecules with proton affinities higher than ammonia form an ion pair complex, which is in good agreement with the present results.^{21,34,35}

As for the HB complexes, the optimized geometries of the IP structures are similar with the 5T and 7T:63T clusters. Again, it is remarkable that, in all cases except CH₂NH, the oxygen atoms of the zeolite framework involved in the hydrogen bond interactions are those bonded to aluminum, independently of the model used. This is in contrast to what is observed for chabazite,⁵⁰ for which the oxygens involved in the hydrogen bonds change upon enlarging the size of the cluster. It should be noted, however, that chabazite has a smaller ring (eight-membered) than MFI (10-membered). The main differences between the 5T and 7T:63T optimized geometries have the same origin and effect than those reported for the less basic molecules. That is, 5T cluster leads always to almost two equivalent hydrogen bonds between the HBase⁺ and Z[−], whereas with the largest 7T:63T cluster, one of the hydrogen bonds is considerably longer due to the existence of zeolite constraints. For the more basic molecules, methylamine and dimethylamine, only the IP structure has been obtained as a minimum. Thus, present results seem to indicate that both 5T and 7T:63T models lead to similar structures when equivalent complexes are found, but they do not always yield to the same number of minima, especially when ion pair structures are involved.

With respect to the interaction energies for HB complexes, both 5T and 7T:63T models provide similar values (see Table 2). With the exception of CH₂NH, for which a new weak hydrogen-bond interaction appears upon enlarging the cluster, adsorption energies computed with the 5T and 7T:63T models differ at the most by 2.5 kcal mol^{−1}. The average factor $f = E_{7\text{T}:63\text{T}}/E_{5\text{T}}$ is 1.1. Thus, present results seem to indicate that



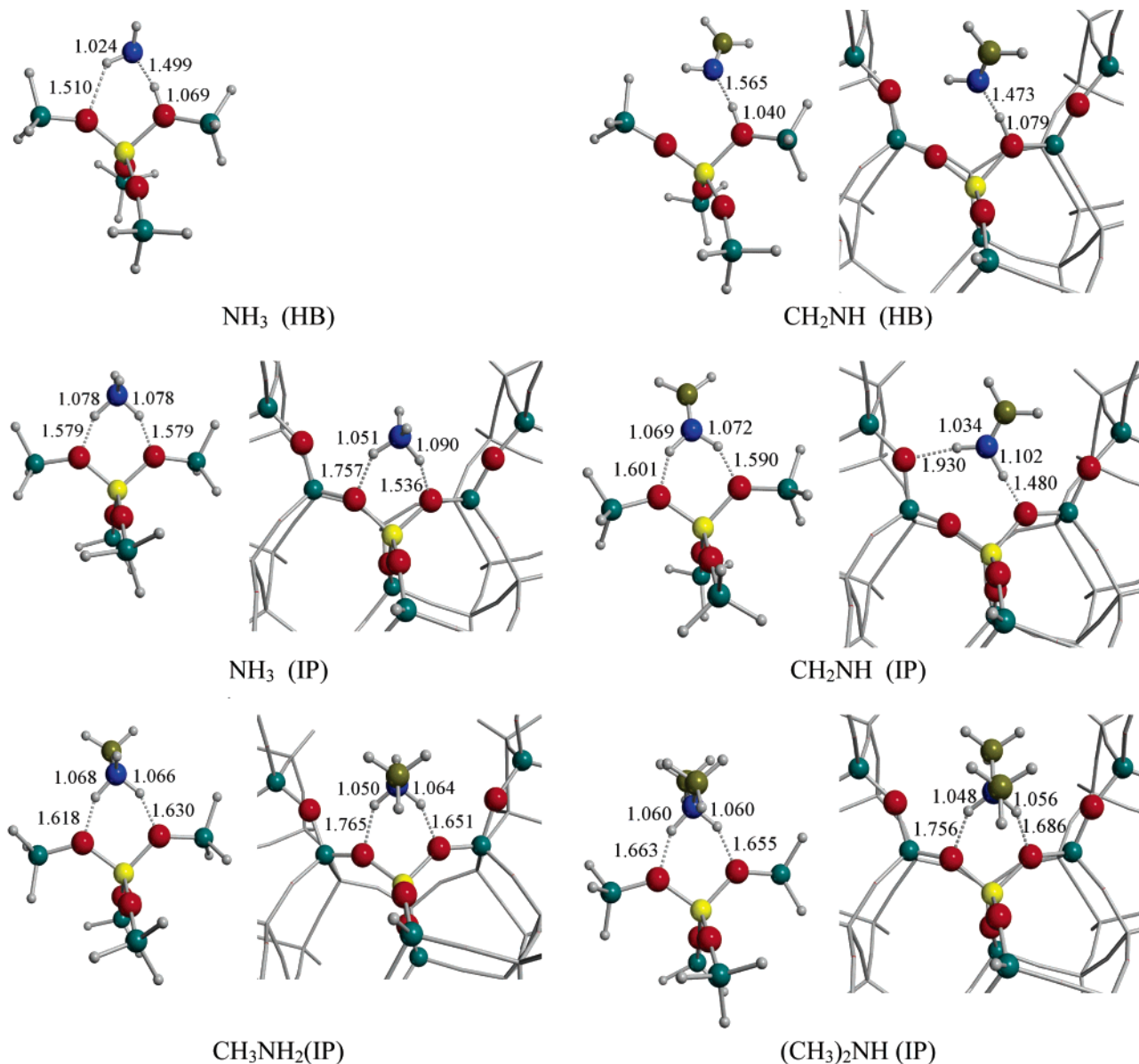


Figure 2. Main geometry parameters of base-HZ complexes using (a) the 5T cluster and the B3LYP/6-31++G(d,p) level of theory and (b) the ONIOM2 7T:63T cluster with the B3LYP/6-31++G(d,p):MNDO methods combination. (Distances are in Å).

TABLE 2: Proton Affinities (PA) and Base-HZ Adsorption Energies (in kcal mol⁻¹)

	hydrogen bonded (HB)				ion pair (IP)			
	5T	7T:63T	<i>f</i> ^a	exp.	7T:63T	<i>f</i> ^a	exp.	
CO	-4.6	-5.1	1.1	6.3 ^b				
H ₂ O	-16.3	-16.9	1.0	21.5 ^c				
CH ₃ OH	-17.0	-18.6	1.1	27.5 ^c				
CH ₃ CHO	-13.7	-15.1	1.1					
CH ₃ CN	-12.9	-12.6	1.0	26.3 ^c				
CH ₃ OCH ₃	-14.3	-16.8	1.2					
NH ₂ CHO	-21.5	-21.4	1.0					
CH ₃ COCHCH ₂	-14.0	-14.7	1.1					
NH ₃	-19.0				-19.5	-27.4	1.4	34.7 ^d
CH ₂ NH	-17.2	-21.7	1.3		-15.8	-26.5	1.7	
CH ₃ NH ₂					-24.0	-33.8	1.4	44.3 ^d
(CH ₃) ₂ NH					-26.9	-38.1	1.4	49.0 ^d

^a $f = (E_{\text{ads}}(7\text{T}:63\text{T})) / (E_{\text{ads}}(5\text{T}))$. ^b Reference 56. ^c Reference 57. ^d Reference 58.

5T cluster is reasonably accurate to describe the formation of hydrogen-bonded complexes in medium-sized channel zeolites,

as it leads to appropriate geometrical parameters and similar adsorption energies to those of more accurate models.

In contrast, the 5T adsorption energies of ion pair systems are significantly underestimated with respect to those obtained with the largest cluster, the smallest difference being 7.9 kcal mol⁻¹. Within the same family of molecules, the underestimation appears to be proportional to the adsorption energy, the higher differences being observed for more basic molecules which present stronger interactions with the zeolite. A constant $f = E_{7\text{T}:63\text{T}}/E_{5\text{T}}$ ratio of 1.4 is determined for amines and a factor $f = 1.7$ for the CH₂NH imine. Overall, a factor (f) of 1.4 should reasonably account for long-range effects in IP structures.

The comparison with the adsorption energies measured in ZSM5 with microcalorimetry techniques reveals that the computed values are lower than those determined experimentally (see Table 2).⁵⁶⁻⁵⁸ The deviation between computed and measured values seems proportional because a quite constant $E_{\text{exp}}/E_{\text{calc}}$ ratio is obtained, with the exception of acetonitrile, which shows an enormous difference difficult to understand. It should be mentioned that these discrepancies between theory and experiments have been largely reported in the literature,

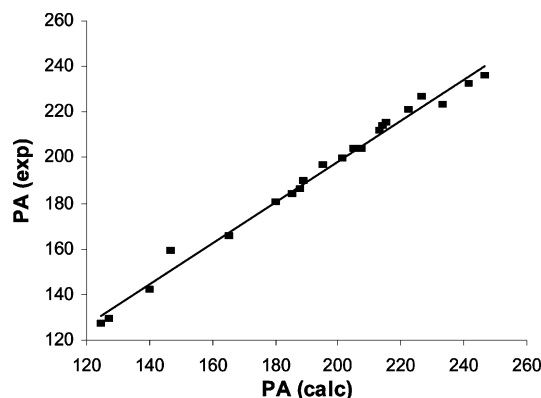


Figure 3. Linear correlation between experimentally and computed proton affinities (in $\text{kcal}\cdot\text{mol}^{-1}$). $PA(\text{exp}) = 0.9004 PA(\text{calc}) + 18.223$; $R^2 = 0.988$.

the computed values usually being smaller than the experimental ones. The higher computed values are obtained with similar or more accurate approximations^{22,59–62} and are similar to those computed in the present work. Moreover, it should be mentioned that microcalorimetry experiments are not able to differentiate, among all the interactions that can be established inside the framework, the acid–base interactions with the Brønsted sites. In particular, although Lewis centers are much more rare, it has been suggested that the interaction of probe molecules with these sites are normally stronger and might affect the final reported values.⁶³

In conclusion, the 5T cluster reproduces reasonably well the structure of the HB and IP complexes but largely underestimates the adsorption energy of the IP ones due to long-range effects. The limitations of the 5T model are more dramatic when the proton affinity of the probe molecule lies in the 204–220 $\text{kcal}\cdot\text{mol}^{-1}$ range because both minima (HB and IP) are obtained with similar stabilities, whereas the largest clusters provides the IP complex to clearly be the ground-state structure, in agreement with experiments.^{21,34,35} The adsorption energies obtained with the 7T:63T cluster are in the range of the most accurate computed values and only somewhat underestimated with

respect to calorimetric measurements. Moreover, it has been shown in a previous study⁵⁰ that similar ONIOM combinations lead to almost identical results to full periodic DFT calculations in the adsorption of H_2O and NH_3 in HCHA. Thus, we expect that the 7T:63T cluster is a reasonably accurate model, and hereafter, the adsorption energies computed with 5T will be corrected by the scale factors $f = 1.1$ for HB and $f = 1.4$ for IP structures.

It is worth noting that when these scale factors are applied to the adsorption energies obtained through the 5T model, the three subsets mentioned at the beginning of our discussion reduce, in practice, to only two because, in all those cases where the 5T model predicts the existence of both HB and IP forms, the latter is strongly favored over the former when the scaling is applied (see Table 1). This implies that the zeolite cavity creates an environment that clearly favors proton transfer. Actually, as we have mentioned above, for the particular case of ammonia, the HB and IP complexes differ by $0.5\text{ kcal}\cdot\text{mol}^{-1}$ in favor of the latter when the 5T model is used, but when a more realistic description of the zeolite is used, only the PT conformation is found. This finding can be considered a manifestation of a more general behavior in which the perturbation of the HB donor (or the HB acceptor, or both) has an important effect on the PT process. In a zeolite, the inclusion of the cavity in the model changes the acidity of the Brønsted site and introduces media stabilizing effects of the ion pair. Such perturbation resembles that recently found by a third polar partner¹⁶ in molecular gas phase studies. As a matter of fact, while a $\text{Cl-H}:\text{NH}_3$ dimer is a typical HB complex, the $\text{FH}:\text{Cl}^-\text{H}:\text{NH}_3$ trimer is better described as a $\text{FH}:\text{Cl}^-\text{H}:\text{NH}_3^+$ IP.⁶⁴ Similarly, spontaneous proton transfer has been predicted for some dimers between phosphinic acid derivatives¹⁵ because, in these complexes, the two monomers behave simultaneously as HB donor and as HB acceptor. In these cases, the monomer also plays the role of a third polar partner, in the sense that its ability to behave as a proton donor is enhanced because another function within the same monomer behaves simultaneously as a proton acceptor, and vice-versa. Thus, according to this view, we can consider that the zeolite behaves as the proton donor

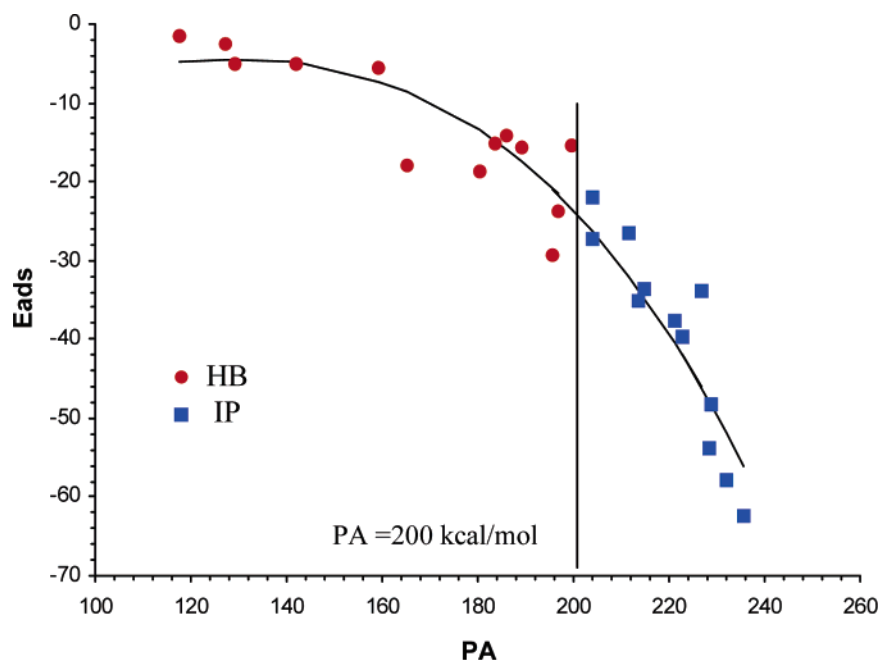


Figure 4. Correlation between adsorption energies and proton affinities (in $\text{kcal}\cdot\text{mol}^{-1}$). $E_{\text{ads}} = -2.02545 \cdot 10^{-5} PA^3 + 5.47943 \cdot 10^{-3} PA^2 - 0.404196 PA$.

and the effect of the cavity plays the role of the third polar partner, in the sense that it significantly favors the PT process.

Correlation Between PAs and Adsorption Energies. One important question that needs to be addressed is whether there is some kind of general correlation between the intrinsic basicity of the base, measured by its gas-phase proton affinity, and the adsorption energies within the zeolite.

For this purpose, we have used the adsorption energies obtained using the 5T model (See Table 1) after scaling them by a factor of 1.1 when the aggregate is HB and by 1.4 when the complex corresponds to an IP. Unfortunately, the experimental PA is known for only 21 out of a total of 25 bases included in our study. On the other hand, a molecule like NO may behave as a N or as an O base within the zeolite, but only its gas-phase PA as a N base is experimentally known. Therefore, to include the whole set in our analysis, we have estimated the four unknown PAs from the correlation found between B3LYP/6-31++G(d,p) calculated values and experimental values for the remaining bases (See Figure 3). This correlation presents an average deviation of about 2 kcal mol⁻¹, excluding F₂CO, for which the deviation is larger. Hence, we can be reasonably confident in the reliability of the values estimated for the unknown PAs.

Figure 4 shows the correlation between scaled adsorption energies and calculated PA's. It can be seen that the different points fit reasonably well to a third degree polynomial. It is not surprising to observe some scatter in the points because we are dealing with small differences, probably beyond the accuracy of the model used. However, it is very important to note that there is a quite clear-cut difference between HB and IP aggregates, which indicates that, in general for bases with PA greater than 200 kcal mol⁻¹, the IP form is favored, and for bases with PA smaller than this value, the HB form should be found.

Conclusions

The interaction of a large set of bases covering a wide range of the basicity scale with HZSM5 medium-sized zeolites has been investigated through the use of two model clusters, namely 5T and 7T:63T. The optimized geometries of the different HB and IP complexes obtained with both models are rather similar. However, there are significant dissimilarities as far as the adsorption energies are concerned, in particular when dealing with IP clusters whose intrinsic stability is largely underestimated when the simpler 5T model is used. 5T clusters could be used to obtain reasonable estimates of adsorption energies, provided these are scaled by a factor of 1.1 for HB complexes and of 1.4 for IP complexes.

The adsorption energies obtained with the 7T:63T cluster are in nice agreement with the most accurate computed values reported in the literature, although they underestimate the calorimetric measurements.

From our results, we can also conclude that the zeolite cavity plays a similar role as third polar partners in gas-phase HB trimers, in the sense that cavity effects significantly favor the PT process.

Interestingly, the intrinsic basicity of the base and its adsorption energy within the zeolite are correlated. From this correlation, it is possible to conclude that, in general, bases with PA larger than 200 kcal mol⁻¹ should lead to the formation of IPs, whereas bases with PA smaller than this value should form HB complexes.

Acknowledgment. This work has been partially supported by the DGI Projects nos. BQU2003-00894, 01251 and BQU2002-

04112-C02. A generous allocation of computational time at the CCC of the Universidad Autónoma de Madrid and the Catalonia Supercomputer Center (CESCA) is also gratefully acknowledged.

Supporting Information Available: Optimized geometries (Cartesian coordinates) of the HZ and B-HZ aggregates obtained with the 5T cluster. This material is available free of charge via the Internet at <http://pubs.acs.org>.

References and Notes

- (1) Bürgi, H.-B.; Dunitz, J. D. *Acc. Chem. Res.* **1983**, *16*, 153.
- (2) Desiraju, G. R.; Steiner, T. *The Weak Hydrogen Bond in Structural Chemistry and Biology*; Oxford Science Publications: Oxford, 1999.
- (3) Alkorta, I.; Rozas, I.; Mó, O.; Yáñez, M.; Elguero, J. *J. Phys. Chem. A* **2001**, *105*, 7481.
- (4) Legon, A. C. *Chem. Soc. Rev.* **1993**, 153.
- (5) Barnes, A. J.; Wright, M. P. *J. Chem. Soc., Faraday Trans. 2* **1986**, *80*, 465.
- (6) Legon, A. C.; Rego, C. A. *J. Chem. Phys.* **1989**, *90*, 6867.
- (7) Legon, A. C.; Wallwork, A. L.; Rego, C. A. *J. Chem. Phys.* **1990**, *92*, 6397.
- (8) Heidrich, D.; van Eikema Homes, J. R.; Schleyer, P. v. R. *J. Comput. Chem.* **1993**, *14*, 1149.
- (9) Legon, A. C. *J. Chem. Soc., Faraday Trans.* **1995**, *91*, 1881.
- (10) Ramos, M.; Alkorta, I.; Elguero, J.; Golubev, N. S.; Denisov, G. S.; Benedict, H.; Limbach, H. H. *J. Phys. Chem. A* **1997**, *101*, 9791.
- (11) Barnes, A. J.; Legon, A. C. *J. Mol. Struct.* **1998**, *448*, 101.
- (12) Alkorta, I.; Elguero, J. *J. Phys. Chem. A* **1999**, *103*, 272.
- (13) Jordan, M. J. T.; Del Bene, J. E. *J. Am. Chem. Soc.* **2000**, *122*, 2101.
- (14) Rozas, I.; Alkorta, I.; Elguero, J. *J. Am. Chem. Soc.* **2000**, *122*, 11154.
- (15) Mó, O.; Yáñez, M.; González, L.; Elguero, J. *ChemPhysChem* **2001**, *7*, 465.
- (16) Hunt, S. W.; Higgins, K. J.; Craddock, M. B.; Brauer, C. S.; Leopold, K. R. *J. Am. Chem. Soc.* **2003**, *125*, 13850.
- (17) Raczynska, E. D.; Decouzon, M.; Gal, J.-F.; Maria, P.-C.; Wozniak, K.; Kurg, R.; Carins, S. N. *Trends Org. Chem.* **1998**, *7*, 95.
- (18) Maksic, Z. B.; Kovacevic, B. *J. Phys. Chem. A* **1999**, *103*, 6678.
- (19) Maksic, Z. B.; Glasovac, Z.; Despotovic, I. *J. Phys. Org. Chem.* **2002**, *15*, 499.
- (20) Sauer, J. *Chem. Rev.* **1989**, *89*, 199.
- (21) Pazé, C.; Bordiga, S.; Lamberti, C.; Salvalaggio, M.; Zecchina, A.; Bellussi, G. *J. Phys. Chem. B* **1997**, *101*, 4740.
- (22) Benco, L.; Demuth, T.; Hafner, J.; Hutschka, F. *Chem. Phys. Lett.* **2000**, *324*, 373.
- (23) Xu, M.; Wang, W.; Hunger, M. *Chem. Commun.* **2003**, 722.
- (24) Baba, T.; Komatsu, N.; Ono, Y.; Sugisawa, H.; Takahashi, T. *Microporous Mesoporous Mater.* **1998**, *22*, 203.
- (25) Sarv, P.; Tuherm, T.; Lippmaa, E.; Keskinen, K.; Root, A. *J. Phys. Chem.* **1995**, *99*, 13763.
- (26) Ryder, J. A.; Chakraborty, A. K.; Bell, A. T. *J. Phys. Chem. B* **2000**, *104*, 6998.
- (27) Fermann, J. T.; Blanco, C.; Auerbach, S. *J. Chem. Phys.* **2000**, *112*, 6779.
- (28) Hölderich, W.; Hesse, M.; Nümann, F. *Angew. Chem., Int. Ed. Engl.* **1988**, *27*, 226.
- (29) Sen, S. E.; Smith, S. M.; Sullivan, K. A. *Tetrahedron* **1999**, *55*, 12657.
- (30) Corma, A. *Chem. Rev.* **1995**, *95*, 559.
- (31) Farneth, W. E.; Gorte, R. J. *Chem. Rev.* **1995**, *95*, 615.
- (32) Gorte, R. J. *Catal. Lett.* **1999**, *62*, 1.
- (33) Auroux, A. *Top. Catal.* **1997**, *4*, 71.
- (34) Gorte, R. J.; White, D. *Top. Catal.* **1997**, *4*, 57.
- (35) Paukshits, E. A.; Malyvsheva, L. V.; Stepanov, V. G. *React. Kinet. Catal. Lett.* **1998**, *65*, 145.
- (36) Maseras, F.; Morokuma, K. *J. Comput. Chem.* **1995**, *16*, 1170.
- (37) Dapprich, S.; Komáromi, I.; Byun, K. S.; Morokuma, K.; Frisch, M. J. *THEOCHEM* **1999**, *461-462*, 1.
- (38) Vreven, T.; Morokuma, K. *J. Comput. Chem.* **2000**, *21*, 1419.
- (39) Solans-Monfort, X.; Bertran, J.; Branchadell, V.; Sodupe, M. *J. Phys. Chem. B* **2002**, *106*, 10220.
- (40) Atoguchi, T.; Yao, S. *J. Mol. Catal. A: Chem.* **2003**, *191*, 281.
- (41) Bobuatong, K.; Limtrakul, J. *Appl. Catal., A* **2003**, *253*, 49.
- (42) Boronat, M.; Viruela, P. M.; Corma, A. *J. Am. Chem. Soc.* **2004**, *126*, 3300.
- (43) Damin, A.; Bordiga, S.; Zecchina, A.; Lamberti, C. *J. Chem. Phys.* **2002**, *117*, 226.

- (44) Jiang, N.; Yuan, S.; Wang, J.; Jiao, H.; Qin, Z.; Li, Y.-W. *J. Mol. Catal. A: Chem.* **2004**, *220*, 221.
- (45) Kasuriya, S.; Namuangruk, S.; Treesukol, P.; Tirtowidjojo, M.; Limtrakul, J. *J. Catal.* **2003**, *219*, 320.
- (46) Namuangruk, S.; Pantu, P.; Limtrakul, J. *J. Catal.* **2004**, *225*, 523.
- (47) Rungsirisakun, R.; Jansang, B.; Pantu, P.; Limtrakul, J. *J. Mol. Struct.* **2004**, *733*, 239.
- (48) Sillar, K.; Burk, P. *J. Phys. Chem. B* **2004**, *108*, 9893.
- (49) Sillar, K.; Burk, P. *Chem. Phys. Lett.* **2004**, *393*, 285.
- (50) Solans-Monfort, X.; Sodupe, M.; Branchadell, V.; Sauer, J.; Orlando, R.; Ugliengo, P. *J. Phys. Chem. B* **2005**, *109*, 3539.
- (51) Becke, A. D. *J. Chem. Phys.* **1993**, *98*, 5648.
- (52) Lee, C.; Yang, W.; Parr, R. G. *Phys. Rev. B* **1988**, *37*, 785.
- (53) Hehre, W. J.; Ditchfield, R.; Pople, J. A. *J. Chem. Phys.* **1972**, *56*, 2257.
- (54) Dewar, M. J. S.; Thiel, W. *J. Am. Chem. Soc.* **1977**, *99*, 4899.
- (55) Frisch, M. J.; Trucks, G. W.; Schlegel, H. B.; Scuseria, G. E.; Robb, M. A.; Cheeseman, J. R.; Zakrzewski, V. G.; Montgomery, J. A., Jr.; Stratmann, R. E.; Burant, J. C.; Dapprich, S.; Millam, J. M.; Daniels, A. D.; Kudin, K. N.; Strain, M. C.; Farkas, O.; Tomasi, J.; Barone, V.; Cossi, M.; Cammi, R.; Mennucci, B.; Pomelli, C.; Adamo, C.; Clifford, S.; Ochterski, J.; Petersson, G. A.; Ayala, P. Y.; Cui, Q.; Morokuma, K.; Malick, D. K.; Rabuck, A. D.; Raghavachari, K.; Foresman, J. B.; Cioslowski, J.; Ortiz, J. V.; Stefanov, B. B.; Liu, G.; Liashenko, A.; Piskorz, P.; Komaromi, I.; Gomperts, R.; Martin, R. L.; Fox, D. J.; Keith, T.; Al-Laham, M. A.; Peng, C. Y.; Nanayakkara, A.; Gonzalez, C.; Challacombe, M.; Gill, P. M. W.; Johnson, B. G.; Chen, W.; Wong, M. W.; Andres, J. L.; Head-Gordon, M.; Replogle, E. S.; Pople, J. A. *Gaussian 98*; Gaussian, Inc.: Pittsburgh, PA, 1998.
- (56) Savitz, S.; Myers, A. L.; Gorte, R. J. *J. Phys. Chem. B* **1999**, *103*, 3687.
- (57) Lee, C.-C.; Gorte, R. J.; Farneth, W. E. *J. Phys. Chem. B* **1997**, *101*, 3811.
- (58) Lee, C.; Parrillo, D. J.; Gorte, R. J.; Farneth, W. E. *J. Am. Chem. Soc.* **1996**, *118*, 3262.
- (59) Nusterer, E.; Blöchl, P. E.; Schwarz, K. *Chem. Phys. Lett.* **1996**, *253*, 448.
- (60) Vollmer, J. M.; Stefanovich, E. V.; Truong, T. N. *J. Phys. Chem. B* **1999**, *103*, 9415.
- (61) Demuth, T.; Benco, L.; Hafner, J.; Toulhoat, H. *Int. J. Quantum Chem.* **2001**, *84*, 110.
- (62) Tuma, C.; Sauer, J. *Chem. Phys. Lett.* **2004**, *387*, 388.
- (63) Busco, C.; Barbaglia, A.; Broyer, M.; Bolis, V.; Foddanu, G. M.; Ugliengo, P. *Thermochim. Acta* **2004**, *418*, 3.
- (64) M6, O.; Yáñez, M.; Del Bene, J. E.; Alkorta, I.; Elguero, J. *ChemPhysChem.* **2005**, *67*, 1411.